

*This thesis is
Dedicated to my
Beloved Parents,
Sister
And
My Respected Supervisors
For Their Constant Inspiration, Whole Hearted
Cooperation and Proper Valuable Guidance*



The Report is Generated by DrillBit Plagiarism Detection Software

Submission Information

Author Name Debadrita Roy
Title INVESTIGATION OF DIVERGENT INTERACTIONS OF SOME
NOTEWORTHY COMPOUNDS PREVALENT IN HOST GUEST AND
SOLUTION CHEMISTRY FOR ENHANCING APPLICABILITY BY
ASSORTED METHODOLOGIES
Paper/Submission ID 1615965
Submitted by nbuplg@nbu.ac.in
Submission Date 2024-04-08 13:15:35
Total Pages 274
Document type Thesis

Result Information

Similarity **0%**

Exclude Information

Quotes Excluded
References/Bibliography Excluded
Sources: Less than 14 Words % Excluded
Excluded Source **16%**
Excluded Phrases Not Excluded

Database Selection

Language English
Student Papers Yes
Journals & publishers Yes
Internet or Web Yes
Institution Repository Yes

A Unique QR Code can be View/Downloaded/Share Pdf File



Signature of Principal Supervisor- *Bimajit Saha* 23-04-2024
Signature of Co-Supervisor- *Subhadeep Saha* 23/04/2024
Signature of the Author- *Debadrita Roy* - 23/04/2024

Dr. Subhadeep Saha, W.B.E.S.
Government of West Bengal
Assistant Professor of Chemistry
Government General Degree College, Pedong

UNIVERSITY OF NORTH BENGAL

Dr. Biswajit Sinha, Ph. D
Professor
Department of Chemistry
E-mail: biswachem@nbu.ac.in
biswachem@gmail.com
M: 9932738973, 9641967211



University of North Bengal
Darjeeling 734 013
West Bengal, India
Ph: +91-353-2776381

Date: April 23, 2024

"समानो मन्त्र समितिः समानी"
Accredited by NAAC with Grade B⁺⁺

CERTIFICATE

I declare that **Ms. Debadrita Roy** has prepared the thesis entitled "**Investigation of Divergent Interactions of Some Noteworthy Compounds Prevalent in Host Guest and Solution Chemistry for Enhancing Applicability by Assorted Methodologies**" for the award of Ph. D degree of University of North Bengal under our joint guidance. She has carried out the work at the Department of Chemistry, University of North Bengal.

Professor
Department of Chemistry
University of North Bengal
Darjeeling -734013, India
Professor & Supervisor

Department of Chemistry
University of North Bengal
Darjeeling-734013
West Bengal, India



**GOVERNMENT GENERAL DEGREE COLLEGE AT PEDONG
DEPARTMENT OF CHEMISTRY**

PO – Pedong, Dist – Kalimpong, West Bengal, India, Pin – 734311
Website: www.pedongcollege.in
Email: chemistryggdcp@gmail.com, pedong.govt.college@gmail.com



सत्यमेव जयते

Date: 23/04/2024

CERTIFICATE

I certify that Ms. Debadrita Roy has prepared the thesis entitled “**INVESTIGATION OF DIVERGENT INTERACTIONS OF SOME NOTEWORTHY COMPOUNDS PREVALENT IN HOST GUEST AND SOLUTION CHEMISTRY FOR ENHANCING APPLICABILITY BY ASSORTED METHODOLOGIES**”, for the award of **Ph.D. (Doctor of Philosophy)** degree from University of North Bengal, under our guidance. She has carried out the work at the Department of Chemistry, University of North Bengal.

Subhadeep Saha

Dr. Subhadeep Saha (W.B.E.S.)
(Co-Supervisor)
Assistant Professor
Department of Chemistry
Government General Degree College at Pedong
Kalimpong – 734311, India

Dr. Subhadeep Saha, W.B.E.S.
Government of West Bengal
Assistant Professor of Chemistry
Government General Degree College, Pedong

DECLARATION

I declare that the thesis entitled “**Investigation of Divergent Interactions of some Noteworthy Compounds Prevalent in Host Guest and Solution Chemistry for Enhancing Applicability by Assorted Methodologies**” has been prepared by me for the Degree of Doctor of Philosophy (Ph.D) under the supervision of Prof. (Dr.) Biswajit Sinha, Professor of Chemistry, University of North Bengal and co-supervision of Dr. Subhadeep Saha (W.B.E.S.), Assistant Professor, Department of Chemistry, Government General Degree College at Pedong, Kalimpong – 734311, India. No part of the thesis has formed the basis for the award of any degree or fellowship previously, in this or any other Institution or University.

Debadrita Roy

DEBADRITA ROY,

Department of Chemistry,
University of North Bengal,
Darjeeling: 734013,
West Bengal, India

DATE: *23/04/2024*

ACKNOWLEDGEMENT

Determination is a crucial prerequisite for accomplishing a goal, which can potentially be performed successfully through proper direction. At this time, I'd like to express my heartfelt gratitude to my respected supervisor, Dr. Biswajit Sinha, Professor, Department of Chemistry, University of North Bengal, West Bengal, India, and my respected co-supervisor, Dr. Subhadeep Saha (W.B.E.S.), Assistant Professor, Department of Chemistry, Government General Degree College at Pedong, Kalimpong - 734311, India. Throughout this challenging path, I have received continual counsel, useful suggestions, motivation, and inspiration from them. They deserve special recognition for not only providing me with his kind direction, but also motivating and encouraging me to go the extra mile along this journey. Without their care and assistance, I would not have been able to complete the thesis in its current shape. I am fortunate to have the opportunity to work under their supervision and would like to express my heartfelt gratitude to them.

I'd also like to thank all of the faculty members at the University of North Bengal's Department of Chemistry for their ongoing enthusiasm and inspiration during my research. I am also grateful to the university authorities, particularly the University Scientific Instrumentation Centre at the University of North Bengal, for providing me the laboratory resources for the study detailed in my thesis.

I specially thank all my lab-mates with whom I worked for their friendly help and encouragement throughout the present investigation.

My gratitude also extends to the sources of the information needed for my research: the countless books, monographs, articles, computer website, etc. I'd want to express my gratitude to individuals whose references I cited in this thesis.

I have to give credit to the people who helped me with this assignment; without their unwavering commitment and collaboration, I could not have finished it. I am deeply grateful to my mother, Smt. Madhabi Roy Isore, father, Dr. Mahendra Nath Roy, and sister, Smt. Madhusree Roy, for their unwavering support throughout these difficult circumstances. All that I am and will become in the future is a result of their immense blessings, dedication to my goals, and selflessness.

Finally, I would like to acknowledge my Respectable Grandfather, Grandmother, Uncle, Aunt and my Dearest Brother and Sister for their boundless and irreparable blessings, inspirations and wishes intending to augment the accomplishment of my Research Work associated with my PhD Thesis.

At last, I would like to thank all my well-wishers and many great people who helped and supported me directly or indirectly throughout this journey.

Debadrita Roy - 23/04/2024

Debadrita Roy

Research Scholar

Department of Chemistry

University of North Bengal

West Bengal, Pin: 734013, India

PREFACE

The research work of my thesis entitled “**Investigation of Divergent Interactions of some Noteworthy Compounds Prevalent in Host Guest and Solution Chemistry for Enhancing Applicability by Assorted Methodologies**” was initiated under the supervision of Dr. Biswajit Sinha, Professor, Department of Chemistry, University of North Bengal, West Bengal, India and co-supervision of Dr. Subhadeep Saha (W.B.E.S.), Assistant Professor, Department of Chemistry, Government General Degree College at Pedong, Kalimpong – 734311, India.

This work deals with the molecular inclusion complexes of cyclic host, oligosaccharide cyclodextrins with various guests like, drug molecules in solid and aqueous environments by various highly sophisticated spectroscopic techniques and physicochemical methods. I also investigated interactions of ionic liquids with bio-active molecules in the solution phase.

During my research work, I have participated in several workshops, conferences and seminars across the country and presented my research work. I was highly inspired by listening and interacting with renowned researchers, experts, reviewers and scientists which helped me a lot in my research work. I was even fortunate enough to publish the works in the thesis in International Journals of repute.

In observance with general practice of reporting scientific observation, due acknowledgement has been made whenever the work described was based on the finding of other investigators. I must take the responsibility of any unintentional omissions and errors, which might have crept in spite of insurances.

LIST OF TABLES

CHAPTER	TABLE	PAGE NUMBER
CHAPTER-IV	Table 1. The detail information about the chemicals	87
	Table 2. Limiting apparent molar volumes (Φ_V^0), Limiting molar refraction (R_M^0), experimental slopes (S_V^*), viscosity A , B -coefficients of (Tartrazine+BTMAC+H ₂ O), (Tartrazine+BTEAC+H ₂ O) and (Tartrazine+BTBAC+H ₂ O) Systems in an aqueous solution of ILs of different molality/mol kg ⁻¹ and at different temperatures and pressure at 1.013 bar	87
	Table 3. The empirical coefficient values (a_0 , a_1 and a_2) of (Tartrazine+BTMAC+H ₂ O), (Tartrazine+BTEAC+H ₂ O) and (Tartrazine+BTBAC+H ₂ O) Systems in different concentrations of the ILs (BTMAC), (BTEAC) & (BTBAC) (0.001, 0.003, 0.005) molality /mol kg ⁻¹ at 298.15K, 308.15K and 318.15K and pressure at 1.013 bar	89
	Table 4. Values of limiting molar expansibilities (Φ_E^0) along with $(\delta\Phi_E^0/\delta T)_P$ for (Tartrazine+BTMAC+H ₂ O), (Tartrazine+BTEAC+H ₂ O) and (Tartrazine+BTBAC+H ₂ O) Systems in different concentration of the ILs (BTMAC), (BTEAC) & (BTBAC) (0.001, 0.003, 0.005) molality/mol kg ⁻¹ at 298.15 K, 308.15 K and 318.15 K and pressure at 1.013 bar	90
	Table 5. Viscosity dB/dT values for (Tartrazine+BTMAC+H ₂ O), (Tartrazine+BTEAC+H ₂ O), (Tartrazine+BTBAC+H ₂ O) systems in different concentrations of ILs at (298.15, 308.15 and 318.15) K and pressure at 1.013 bar	90
	Table 6. Values of (B/Φ_V^0) for (Tartrazine+BTMAC+H ₂ O), (Tartrazine+BTEAC+H ₂ O) and (Tartrazine+BTBAC+H ₂ O) Systems in different molality (mol kg ⁻¹) of aqueous solution of IL	91

CHAPTER	TABLE	PAGE NUMBER
	(BTMAC, BTEAC & BTBAC) mixture at different temperatures and atmospheric pressure 1.013 bar	
	Table 7. Values of $(\bar{V}_1^0 - \bar{V}_2^0)$, $\Delta\mu_1^{0\#}$, $\Delta\mu_2^{0\#}$, $T\Delta S_2^{0\#}$, $\Delta H_2^{0\#}$ for (Tartrazine+BTMAC+H ₂ O), (Tartrazine+BTEAC+H ₂ O) and (Tartrazine+BTEAC+H ₂ O) Systems in different molality (mol/kg) of aqueous solution of IL (BTMAC, BTEAC & BTBAC) mixture at different temperatures and atmospheric pressure 1.013 bar	92
	Table 8. Molar conductance (Λ) of (Tartrazine + BTMAC + H ₂ O), (Tartrazine + BTEAC + H ₂ O), (Tartrazine + BTBAC + H ₂ O) systems in aqueous ILs solution in (0.001, 0.003, 0.005) molality /mol kg ⁻¹ at 298.15 K, 308.15 K and 318.15 K and pressure at 1.013 bar	93
	Table 9. Limiting molar conductance (Λ_0) of (Tartrazine+BTMAC+H ₂ O), (Tartrazine+BTEAC+H ₂ O), (Tartrazine+BTBAC+H ₂ O) systems in aqueous ILs solution in (0.001, 0.003, 0.005) molality /mol kg ⁻¹ at 298.15 K, 308.15 K and 318.15 K and pressure at 1.013 bar	94
	Table 10. Surface Tension (σ) values of (Tartrazine + Aq. BTMAC), (Tartrazine+ Aq. BTEAC (Tartrazine+Aq.BTBAC) systems in ionic liquids solutions at different concentration (0.001 ,0.003 ,0.005) mol kg ⁻¹ at 298.15 K and pressure at 1.013 bar	95
	Table 11. Limiting Slopes ($\partial\sigma/\partial m$) and intercept of the Surface Tension of (Tartrazine+BTMAC+H ₂ O), (Tartrazine+BTEAC+H ₂ O), (Tartrazine+BTBAC+H ₂ O) systems in aqueous solutions of ILs of different molality at 298.15K	97
	Table 12. ΔH° (kJ mol ⁻¹), ΔS° (kJ mol ⁻¹ K ⁻¹), and ΔG° (kJ mol ⁻¹) for the (a) Tartrazine+BTMAC (b) Tartrazine+BTEAC (c) Tartrazine+BTBAC	97
	Table S1. Density (ρ), viscosity (η) and molar refraction (R_M) of Azo dye Tartrazine in aqueous BTMAC ionic liquid solutions at 298.15	98

CHAPTER	TABLE	PAGE NUMBER
	K, 308.15 K and 318.15 K and pressure at 1.013 bar	
	Table S2. Density (ρ), viscosity (η) and molar refraction (R_M) of Azo dye Tartrazine in aqueous BTEAC ionic liquid solutions at 298.15 K, 308.15 K and 318.15 K and pressure at 1.013 bar	99
	Table S3. Density (ρ), viscosity (η) and molar refraction (R_M) of Azo dye Tartrazine in aqueous BTBAC ionic liquid solutions at 298.15 K, 308.15 K and 318.15 K and pressure at 1.013 bar	100
	Table S4. Apparent molar volume, (Φ_V) and $(\eta/\eta^0-1)/\sqrt{c}$ of (Tartrazine+BTMAC+H ₂ O) system in (0.001 , 0.003, 0.005) mol kg ⁻¹ aqueous BTMAC solution at different temperatures 298.15 K, 308.15 K, 318.15 K and pressure at 1.013 bar	101
	Table S5. Apparent molar volume, (Φ_V) and $(\eta/\eta^0-1)/\sqrt{c}$ of (Tartrazine +BTEAC +H ₂ O) system in (0.001 , 0.003 , 0.005) mol kg ⁻¹ in aqueous (BTEAC) solution at different temperatures 298.15 K, 308.15 K, 318.15 K and pressure at 1.013 bar	103
	Table S6. Apparent molar volume, (Φ_V) and $(\eta/\eta^0-1)/\sqrt{c}$ of (Tartrazine+BTBAC+H ₂ O) system in (0.001 , 0.003 , 0.005) mol kg ⁻¹ in aqueous (BTBAC) solution at different temperatures 298.15 K, 308.15 K, 318.15 K and pressure at 1.013 bar	104
	Table S7. Refractive index (n_D) and specific conductance (κ) of (Tartrazine + Aq. BTMAC) system in aqueous IL (BTMAC) solution at 298.15 K, 308.15 K and 318.15 K and pressure at 1.013 bar	105
	Table S8. Refractive index (n_D) and specific conductance (κ) of (Tartrazine + Aq. BTEAC) system in aqueous IL (BTEAC) solution at 298.15 K, 308.15 K and 318.15 K and pressure at 1.013 bar	106

CHAPTER	TABLE	PAGE NUMBER
	Table S9. Refractive index (n_D) and specific conductance (κ) of (Tartrazine + Aq. BTBAC) system in aqueous IL (BTBAC) solution at 298.15 K, 308.15 K and 318.15 K and pressure at 1.013 bar	107
	Table S10. UV-Vis Spectroscopic data for the Benesi-Hildebrand double reciprocal plot of (Tartrazine+Aq.BTMAC) system at 298.15 K	108
	Table S11 UV-Vis Spectroscopic data for the Benesi-Hildebrand double reciprocal plot of (Tartrazine+Aq.BTEAC) system at 298.15 K	109
	Table S12. UV-Vis Spectroscopic data for the Benesi-Hildebrand double reciprocal plot of (Tartrazine+Aq.BTBAC) system at 298.15 K	109
CHAPTER-V	Table 1. Specification of chemical samples	142
	Table 2. Limiting apparent molar volumes(Φ_V^0), Limiting molar refraction(R_M^0), experimental slopes (S_V^*), viscosity A, B-coefficients of L-Asparagine solution in IL (BTMAC) at different temperatures and pressure at 1.013bar	142
	Table 3. Limiting apparent molar volumes(Φ_V^0), Limiting molar refraction(R_M^0), experimental slopes (S_V^*), viscosity A, B-coefficients of L-Asparagine solution in IL (BTEAC) at different temperatures and pressure at 1.013bar	143
	Table 4. The empirical coefficient values (a_0 , a_1 and a_2) of L-Asparagine solution in different molality of the ILs (BTMAC) & (BTEAC) (0.001,0.003,0.005) at 298.15K, 303.15K and 308.15K and pressure at 1.013bar	144
	Table 5. Values of limiting molar expansibilities (Φ_E^0) for L-Asparagine solution in IL (BTMAC) at different temperatures and pressure at 1.013bar	144
	Table 6. Values of limiting molar expansibilities (Φ_E^0) for L-Asparagine solution in IL (BTEAC) at different temperatures and pressure at 1.013bar	145
	Table 7. Viscosity B-coefficients of L-Asparagine solution along with dB/dT values in different	145

CHAPTER	TABLE	PAGE NUMBER
	molality of IL (BTMAC) at (298.15, 303.15 and 308.15) K and pressure at 1.013bar	
	Table 8. Viscosity B-coefficients of L-Asparagine solution along with dB/dT values in different molality of IL (BTEAC) at (298.15, 303.15 and 308.15) K and pressure at 1.013bar	146
	Table 9. Values of (B/Φ_v^0) for L-Asparagine in different molality of aqueous BTMAC and BTEAC (IL) solutions at different temperature and atmospheric pressure 1.013bar	146
	Table 10. Values of $(\bar{v}_1^0 - \bar{v}_2^0)$, $\Delta\mu_1^{0\#}$, $\Delta\mu_2^{0\#}$, $T\Delta S_2^{0\#}$, $\Delta H_2^{0\#}$ for L-Asparagine in different molality(m) of aqueous solution of IL(BTMAC&BTEAC) mixture at different temperatures and atmospheric pressure 1.013 bar	147
	Table 11. Molar conductance (Λ) of L-Asparagine solutions in aqueous BTMAC & BTEAC ionic liquid solution in different molality (0.001, 0.003, 0.005) at 298.15K, 303.15K and 313.15K and pressure at 1.013bar	148
	Table 12. Surface Tension (σ) values of L-Asparagine solutions in IL (BTMAC) and L-Asparagine solutions in IL (BTEAC) at different molality(0.001,0.003,0.005) at room temperature and pressure at 1.013bar	149
	Table 13. Limiting Slopes ($\partial\sigma/\partial m$) of the Surface Tension of the Aqueous Solutions of α -Amino acid	149
	Table S1. Experimental values of density (ρ), viscosity (η) and molar refraction (R_M) of different molality (m) of aqueous IL (BTMAC) solution at 298.15K, 303.15K and 308.15K and pressure at 1.013bar	150
	Table S2. Experimental values of density (ρ), viscosity (η) and molar refraction (R_M) of different molality (m) of aqueous IL (BTEAC) solution at 298.15K, 303.15K and 308.15K. and pressure at 1.013bar	150
	Table S3. Experimental values of refractive index (n_D) and specific conductance (κ) of	151

CHAPTER	TABLE	PAGE NUMBER
	different molality (m) of aqueous IL (BTMAC) solution at 298.15 K, 303.15 K and 308.15 K and pressure at 1.013bar	
	Table S4. Experimental values of refractive index (n_D) and specific conductance (κ) of different molality (m) of aqueous IL (BTEAC) solution at 298.15 K, 303.15 K and 308.15 K. and pressure at 1.013bar	151
	Table S5. Density (ρ), viscosity (η) and molar refraction (R_M) of L-Asparagine in aqueous (BTMAC)ionic liquid solutions at 298.15K, 303.15K and 308.15K and pressure at 1.013bar	152
	Table S6. Density (ρ), viscosity (η) and molar refraction (R_M) of L-Asparagine in aqueous (BTEAC)ionic liquid solutions at 298.15K, 303.15K and 308.15K. and pressure at 1.013bar	153
	Table S7. Apparent molar volume, (Φ_v) and $(\eta/\eta^0 - 1) / \sqrt{m}$ of L-Asparagine solution in (0.001, 0.003, 0.005) different molality in aqueousBTMAC solution at different temperatures 298.15K, 303.15K, 308.15K and pressure at 1.013bar	154
	Table S8. Apparent molar volume, (Φ_v) and $(\eta/\eta^0 - 1) / \sqrt{m}$ of L-Asparagine solutions in (0.001, 0.003 , 0.005) different molality in aqueous(BTEAC) solution at different temperatures 298.15K, 303.15K, 308.15K and pressure at 1.013bar	155
	Table S9. Refractive index (n_D) and specific conductance (κ) of L-Asparagine in aqueous IL (BTMAC)solution at 298.15K, 303.15K and 308.15K and pressure at 1.013bar	156
	Table S10. Refractive index (n_D) and specific conductance (κ) of L-Asparagine in aqueous IL (BTEAC)solution at 298.15K, 303.15K and 308.15K and pressure at 1.013bar	157
CHAPTER-VI	Table 1. Values of Binding affinity (K_a) and Gibb's free energy change (ΔG) for the encapsulation process between BNZ and HP- β -CD	180

CHAPTER	TABLE	PAGE NUMBER
	Table 2. Lowest binding energy of BNZ with HP- β -CD obtained from molecular docking	180
	Table 3. IC ₅₀ values of free BNZ, HP- β -CD and BNZ-HP- β -CD complex for A549 and SKOV3 cancer cell lines	180
	Table 4. Antioxidant activity of BNZ and BNZ-HP- β -CD against the tested free radicals (results presented as mean \pm standard deviation, n=3)	180
	Table S1. Data for the Job plot performed by UV-Visible spectroscopy for aqueous BNZ-HP- β -CD system at 298 K	181
	Table S2. Data for surface tension study of aqueous BNZ-HP- β -CD system at 298 K	181
	Table S3. Values of surface tension (γ) at the break point with corresponding concentrations of HP- β -CD and BNZ at 298 K	182
	Table S4. Data for the Benesi-Hildebrand double reciprocal plot performed by UV-Visible spectroscopy for aqueous BNZ-HP- β -CD system at 298 K	182
	Table S5. ¹ H NMR data of pure BNZ, HP- β -CD and BNZ-HP- β -CD complex	182
	Table S6. Change in FT-IR spectral frequencies of BNZ after complexation with HP- β -CD at room temperature	182
CHAPTER-VII	Table 1. ¹ H NMR data of pure DPAH, α -CD and DPAH+ α -CD inclusion complex	203
	Table 2. FTIR data of pure DPAH, α -CD and DPAH+ α -CD inclusion complex	203
	Table 3. IC ₅₀ values for DPAH and DPAH- α -CD complex	204
CHAPTER-VIII	Table 1. Values of surface tension (γ) at the break point with corresponding concentrations of HP- β -CD and ADP at 298 K	227
	Table 2. Association constant (K _a) obtained by Benesi-Hildebrand method for ADP-HP- β -CD inclusion complex at 298 K	227
	Table 3. IC ₅₀ values for ADP and ADP-HP- β -CD complex	227
	Table 4. Adsorption energy; HOMO, LUMO levels, band gap and other global parameters for	227

CHAPTER	TABLE	PAGE NUMBER
	ADP and ADP-HP- β -CD inclusion complexes in water medium	
	Table S1. ^1H NMR data of pure ADP, HP- β -CD and ADP-HP- β -CD complex	228
	Table S2. FT-IR data of pure ADP, HP- β -CD and ADP-HP- β -CD complex	228
	Table S3. Data for Job plot performed by UV-Visible spectroscopy for aqueous ADP-HP- β -CD system at 298 K.	229
	Table S4. Data for surface tension study of aqueous ADP-HP- β -CD system at 298 K	229
	Table S5. Data for the Benesi-Hildebrand double reciprocal plot performed by UV-Visible spectroscopy for aqueous ADP-HP- β -CD system at 298K	230

LIST OF FIGURES

CHAPTER	FIGURE CAPTION	PAGE NUMBER
Chapter -IV	Figure 1. Variation of Φ_V^0 as a function of molality of ILs as well as the function of temperature where (a) Tartrazine + BTMAC + H ₂ O (b) Tartrazine + BTEAC + H ₂ O (c) Tartrazine + BTBAC + H ₂ O.	110
	Figure 2. dB/dT variations as a function of molality of aqueous ionic liquids.	111
	Figure 3. Variation of R_M^θ with different molality of ionic liquids and different temperatures where (a) Tartrazine + BTMAC + H ₂ O (b) Tartrazine + BTEAC + H ₂ O (C) Tartrazine + BTBAC + H ₂ O.	111
	Figure 4. Variation of Molar conductivity of azo dye with different concentrations at different temperatures and different molality of ionic liquid BTMAC.	112
	Figure 5. Variation of Molar conductivity of azo dye with different concentrations at different temperatures and different molality of ionic liquid BTEAC.	113
	Figure 6. Variation of Molar conductivity of azo dye with different concentrations at different temperatures and different molality of ionic liquid BTBAC.	114
	Figure 7. Surface tension variations with different concentrations of azo dye at different molality of ionic liquid (BTMAC, BTEAC, BTBAC) at 298.15 K.	115
	Figure 8. UV-Vis spectra of (BTMAC+Tartrazine) system.	116

CHAPTER	FIGURE CAPTION	PAGE NUMBER
	Figure 9. UV-Vis spectra of (BTEAC+Tartrazine) system.	116
	Figure 10. UV-Vis spectra of (BTBAC+Tartrazine) system.	117
	Figure 11. Optimized structure for the (a) Tartrazine+BTMAC (b) Tartrazine+BTEAC (c) Tartrazine+BTBAC.	117
	Figure 12. Electrostatic potential map for the (a) Tartrazine+BTMAC (b) Tartrazine+BTEAC (c) Tartrazine+BTBAC.	118
	Figure S1. Benesi double reciprocal plot of BTMAC vs dye tartrazine .	118
	Figure S2. Benesi double reciprocal plot of BTEAC vs dye tartrazine .	119
	Figure S3. Benesi double reciprocal plot of BTBAC vs dye tartrazine .	119
	Figure S4. (a) ^1H NMR of Benzyl tri-methyl ammonium chloride (BTMAC) in D_2O , (b) ^1H NMR of Benzyl tri-ethyl ammonium chloride (BTEAC) in D_2O , (c) ^1H NMR of Benzyl tri-butyl ammonium chloride (BTBAC) in D_2O , (d) ^1H NMR of Tartrazine (TZ) in D_2O , (e) ^1H NMR of Benzyl tri-methyl ammonium chloride (BTMAC)+ Tartrazine (TZ) in D_2O , (f) ^1H NMR of Benzyl tri-ethyl ammonium chloride (BTEAC)+ Tartrazine (TZ) in D_2O , (g) ^1H NMR of Benzyl tri-butyl ammonium chloride (BTBAC)+ Tartrazine (TZ) in D_2O .	123

CHAPTER	FIGURE CAPTION	PAGE NUMBER
Chapter-V	Figure 1. Variation of limiting apparent molar volume (Φ_v^0) of L-Asparagine against different molality (0.001,0.003,0.005)of aqueous BTMAC solutions and function as a function of temperature(T/K)	158
	Figure 2. Variation of limiting apparent molar volume (Φ_v^0) of L-Asparagine against different molality (0.001,0.003,0.005) of aqueous BTEAC solutions and function as a function of temperature(T/K)	158
	Figure 3. Variation of viscosity B-coefficient of L-Asparagine as a function of different temperature(T/K) and different molality of aqueous BTMAC(IL) solutions	159
	Figure 4. Variation of viscosity B-coefficient of L-Asparagine as a function of different temperature(T/K) and different molality of aqueous BTEAC(IL) solutions	159
	Figure 5. Variation of Limiting Molar refraction (R_M^0) of L-Asparagine as a function of temperature (T/K) and different molality (0.001,0.003,0.005) of aqueous BTMAC solutions	160
	Figure 6. Variation of Limiting Molar refraction (R_M^0) of L-Asparagine as a function of temperature (T/K) and different molality (0.001,0.003,0.005) of aqueous BTEAC solutions	160
	Figure 7. Variation of molar conductance (Λ) plot as a function of the concentration of L-Asparagine (amino acid) in 0.001molalityof	161

CHAPTER	FIGURE CAPTION	PAGE NUMBER
	aqueous BTMAC solutions at different temperatures (T/K)	
	Figure 8. Variation of molar conductance (Λ) plot as a function of the concentration of L-Asparagine (amino acid) in 0.003molalityof aqueous BTMAC solutions at different temperatures (T/K)	161
	Figure 9. Variation of molar conductance (Λ) plot as a function of the concentration of L-Asparagine (amino acid) in 0.003molalityof aqueous BTMAC solutions at different temperatures (T/K)	162
	Figure 10. Variation of molar conductance (Λ) plot as a function of the concentration of L-Asparagine (amino acid) in 0.001 molalityof aqueous BTEAC solutions at different temperatures (T/K)	162
	Figure 11. Variation of molar conductance (Λ) plot as a function of the concentration of L-Asparagine (amino acid) in 0.003 molalityof aqueous BTEAC solutions at different temperatures (T/K)	163
	Figure 12. Variation of molar conductance (Λ) plot as a function of the concentration of L-Asparagine (amino acid) in 0.005 molalityof aqueous BTEAC solutions at different temperatures (T/K)	163
	Figure S1. Variation of surface tension (σ) plot of L-Asparagine as a function of different molality of aqueous BTMAC solutions at 298.15 K	164

CHAPTER	FIGURE CAPTION	PAGE NUMBER
	Figure S2. Variation of surface tension (σ) plot of L-Asparagine as a function of different molality of aqueous BTEAC solutions at 298.15 K	164
Chapter-VI	Figure 1. (a) Job plot for BNZ-HP- β -CD system at 298.15 K ($\lambda_{\max} = 270$ nm); (b) Surface tension variation of aqueous BNZ solution with increasing HP- β -CD concentration at 298.15 K.	183
	Figure 2. Benesi-Hildebrand plot for BNZ-HP- β -CD system ($\lambda_{\max} = 270$ nm) at 298.15 K.	183
	Figure 3. FT-IR spectra of HP- β -CD, BNZ, physical mixture and solid BNZ-HP- β -CD inclusion complex.	183
	Figure 4. PXRD diffractograms of HP- β -CD, BNZ, physical mixture and BNZ-HP- β -CD complex (IC).	185
	Figure 5. DSC thermograms of BNZ, HP- β -CD, physical mixture and BNZ-HP- β -CD complex (IC).	186
	Figure 6. Docked conformation of BNZ-HP- β -CD inclusion complex (IC), side view (a) and top view (b) Legend: (a, b) BNZ (guest) is shown as ball-stick, (a) HP- β -CD (host) as stick, (a, b) only polar H-atoms are shown as aqua colored balls and sticks for HP- β -CD and BNZ respectively, (b) HP- β -CD is shown as blue colored 3D surface.	187
	Figure 7. Dose-dependent growth inhibition of (a) lung carcinomic A549 cell line and (b) ovarian SKOV3 cancer cell line after 24 hours of exposure to BNZ, BNZ-HP- β -CD	187

CHAPTER	FIGURE CAPTION	PAGE NUMBER
	complex and HP- β -CD. The obtained results are presented as mean \pm standard deviation of three separate experiments.	
	Figure 8. Inhibition percentage of studied samples at different tested concentrations	188
	Figure S1. ^1H NMR spectra of (a) BNZ, (b) HP- β -CD and (c) BNZ-HP- β -CD complex in D_2O .	189
	Figure S2. 2D ROESY NMR spectra of pure BNZ in D_2O .	190
	Figure S3. 2D ROESY NMR spectra of pure HP- β -CD in D_2O .	190
	Figure S4. 2D ROESY NMR spectra of BNZ-HP- β -CD inclusion complex in D_2O .	191
Chapter-VII	Figure 1. ESI mass spectra of DPAH+ α -CD inclusion complex.	205
	Figure 2. (a) ^1H NMR spectra of pure DPAH and (b) DPAH- α -CD complex and © α -CD.	206
	Figure 3. FT-IR spectra of DPAH, α -CD and DPAH- α -CD complex.	207
	Figure 4. SEM images of (a) DPAH, (b) α -CD and (c) DPAH- α -CD inclusion complex.	208
	Figure 5. DSC thermograms of α -CD, DPAH and DPAH- α -CD complex (IC).	209
	Figure 6. TGA thermograms of DPAH, α -CD and DPAH- α -CD complex (IC).	209
	Figure 7. Cytotoxicity results at different concentrations of DPAH.	210
	Figure 8. Geometry optimization of the molecules at B3LYP/6-31+G(d) level of	210

CHAPTER	FIGURE CAPTION	PAGE NUMBER
	theory. Top and side views of the DPAH- α -CD inclusion complex.	
	Figure 9. Electrostatic potential map for DPAH- α -CD inclusion complex.	211
	Figure 10. Plots of reduced density gradient (RDG) for DPAH- α -CD inclusion complex.	211
Chapter-VIII	Figure 1. 2D ROESY spectra of solid inclusion complex of ADP and HP- β -CD in D ₂ O.	231
	Figure 2. FT-IR spectra of HP- β -CD, ADP and ADP-HP- β -CD complex.	232
	Figure 3. Job plot of ADP+HP- β -CD system at $\lambda_{\max} = 258$ nm at 298 K. $R = [\text{ADP}]/([\text{ADP}] + [\text{HP-}\beta\text{-CD}])$, $\Delta A =$ absorbance difference of ADP without and with HP- β -CD.	233
	Figure 4. Variation of surface tension of aqueous ADP with increasing concentration of HP- β -CD solution at 298 K.	233
	Figure 5. SEM images of (a) ADP, (b) HP- β -CD and (c) ADP+HP- β -CD inclusion complex.	234
	Figure 6. PXRD profiles of HP- β -CD, ADP and ADP-HP- β -CD inclusion complex (IC).	234
	Figure 7. DSC thermograms of ADP, HP- β -CD and ADP-HP- β -CD complex (IC).	235
	Figure 8. TGA thermograms of ADP, HP- β -CD and ADP-HP- β -CD complex (IC).	236
	Figure 9. Pictorial representation of antibacterial activity of the tested samples against the studied microorganisms.	236
	Figure 10. Zone of inhibition against the tested bacteria. Vertical bar above the	237

CHAPTER	FIGURE CAPTION	PAGE NUMBER
	column represent the standard deviation of three replications. Treatments denoted with different letters differ significantly at $p \leq 0.05$ by Tukey's HSD test.	
	Figure 11. Cytotoxicity results at different concentrations of ADP.	237
	Figure 12. Geometry optimization of the molecules at M06-2X-/6-31+G(d) level of theory. Top and side views of the ADP-HP- β -CD.	238
	Figure 13. HOMO and LUMO charge densities of ADP-HP- β -CD inclusion complex	238
	Figure 14. Electrostatic potential map for ADP-HP- β -CD inclusion complex.	239
	Figure 15. Plots of reduced density gradient (RDG) for ADP-HP- β -CD inclusion complex.	239
	Figure S1. ^1H NMR spectra of (a) ADP, (b) HP- β -CD and (c) ADP+HP- β -CD complex in D_2O .	241
	Figure S2. Benesi-Hildebrand double reciprocal plot for the effect of HP- β -CD on the absorbance of ADP (258 nm).	241

LIST OF SCHEMES

CHAPTER	SCHEME	PAGE NUMBER
CHAPTER-IV	Scheme 1. Chemical structures of Benzyl tri-methyl ammonium chloride, Benzyl tri-ethyl ammonium chloride, Benzyl tri-butyl ammonium chloride ILs and Azo dye Tartrazine.	124
	Scheme 2. Representations of different molecular interactions schematically interrelated with three ionic liquids with one azo dye: (1), (4) & (7) (\leftrightarrow) Ion–Ion interactions; (2), (5) & (8) (\leftrightarrow) Ion-Hydrophobic interactions; (3), (6) & (9) (\leftrightarrow) hydrophobic-hydrophobic interactions.	124
CHAPTER-V	Scheme 1. Pictorial representation of solute solvent interaction.	165
	Scheme 2. Plausible molecular interactions existing between the ionic liquids, BTMAC and BTEAC with the amino acid, L-Asparagine.	165
CHAPTER-VI	Scheme 1. Molecular Structures of (a) BNZ and (b) HP- β -CD.	192
CHAPTER-VII	Scheme 1. Molecular structure of DPAH and α -CD.	212
CHAPTER-VIII	Scheme 1. Molecular structures of (a) ADP and (b) HP- β -CD.	242

ABBREVIATIONS

CD	Cyclodextrin
α -CD	α -cyclodextrin
HP- β -CD	2-Hydroxypropyl- β -cyclodextrin
IC	Inclusion complex
BNZ	Benserazide hydrochloride
ADP	Adiphenine hydrochloride
DPAH	D-Pantothenic acid hemicalcium salt
BTBAC	Benzyltributylammonium chloride
BTEAC	Benzyltriethylammonium chloride
BTMAC	Benzyltrimethylammonium chloride
L-Asparagine	L-Asp
TZ	Tartrazine
IL	Ionic liquid
AA	Amino acid
μ m	Micrometre
Å	Angstrom
C	Carbon
H	Hydrogen
O	Oxygen
cm	Centimetre
DMF	Dimethylformamide
DMSO	Dimethyl sulfoxide
EtOH	Ethanol
Eq.	Equation
eV	Electron Volt
Fig.	Figure
ESI-MS	Electron Ionization Spray- Mass Spectrometry
g	Gram
hrs	Hours
Hz	Hertz
FTIR	Fourier Transform Infrared spectroscopy
K	Kelvin

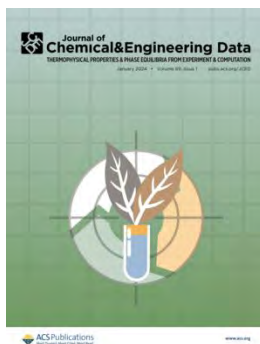
Abbreviations

M	Molar
m	Meter
mg	Milligram
min	Minute
mL	Millilitre
μ M	Micromolar
μ L	Microlitre
NIR	Near Infrared
$^{\circ}$ C	Degree Celsius
pH	Potential of Hydrogen
rpm	Revolutions Per Minute
SEM	Scanning Electron Microscopy
TGA	Thermogravimetric Analysis
DSC	Differential Scanning Calorimetry
UV-vis	Ultraviolet-visible
NMR	Nuclear Magnetic Resonance
XRD	X-Ray Diffraction

APPENDIX A

LIST OF PUBLICATIONS

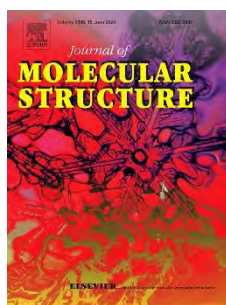
1. Exploration of Solvation Consequences of Ionic Liquids Prevalent in the Aqueous Media of Food Additive Azo Dye Tartrazine by Physicochemical and Computational Studies



J. Chem. Eng. Data 2024, 69, 1, 38–58

(Included in the Thesis)

2. Probing supramolecular complexation of the drug benserazide hydrochloride with hydroxypropyl- β -cyclodextrin by experimental and computational studies



Journal of Molecular Structure, (1294) Part 1, 2023, 136329

(Included in the Thesis)

3. Physicochemical investigation of L-Asparagine in green solvent arrangements with the manifestation of solvation consequences



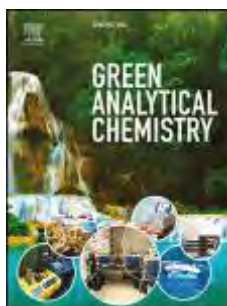
**World Journal of Advanced Research and Reviews, 2022, 13(02), 401–428
(Included in the Thesis)**

4. Exploring 2:1 inclusion complexes of cyclodextrins and antispasmodics, Alverine citrate for enhancing bioavailability and sustained dischargement



Journal of Molecular Liquids, (370), 2023, 121036

5. A green approach towards the removal of a water pollutant by encapsulation of HBCDD into cyclodextrins: Combined experimental and theoretical studies



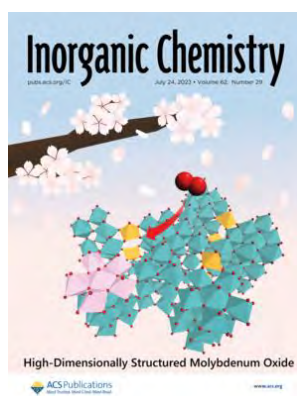
Green Analytical Chemistry,(8), 2024, 100097

6. Synthesis, crystal structure, Hirshfeld surface, and DFT studies of a Copper(II) complex of 5,5'-dimethyl-2,2'-bipyridine and 1,2,2-trimethylcyclopentane-1,3-dicarboxylic acid



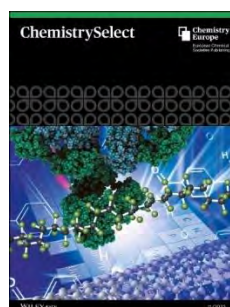
Results in Chemistry,(6), 2023, 101050

7. Label-Free Detection of Epinephrine Using Flower-like Biomimetic CuS Antioxidant Nanozymes



Inorg. Chem. 2023, 62, 29, 11291–11303

8. Molecular Assembly of Rhodanine with Torus-Shaped Cyclodextrins and Their Innovative Applications by Physicochemical Contrivance Simultaneously Optimized by Computational Study



Chem Select, 8, 11,2023,e202300417

9. Fe–Mn nanocomposites doped graphene quantum dots alleviate salt stress of *Triticum aestivum* through osmolyte accumulation and antioxidant defense



Scientific Reports

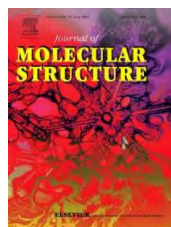
Scientific Reports volume 13, Article number: 11040 (2023)

10. Inclusion of an antiplatelet agent inside into β -cyclodextrin for biochemical applications with diverse authentications



Food Chemistry Advances, Volume 1, October 2022, 100015

11. Encapsulated hydroxychloroquine and chloroquine into cyclic oligosaccharides are the potential therapeutics for COVID-19: insights from first-principles calculations



Journal of Molecular Structure, Volume 1247, 5 January 2022, 131371

List of Seminars/Symposiums/Conferences Attended

- DBT & DST-SERB (Govt. of India) Sponsored International Conference on “Advances in Plants, Microbes and Agricultural Sciences”, Organised by DST (FIST) & UGC-SAP assisted DRS, Department of Botany, University of North Bengal, 2nd –4th March, 2023. (*Best Oral Presentation*)
- International Seminar on Frontiers in Chemistry 2023 & Prof. C. N. R. Rao Endowment Lecture, Department of Chemistry, University of North Bengal, 13-15th March, 2023. (*Presented a Poster*)
- National Conference on “ Environmental Determinism, Diverse Pollutions, Sources, And Controlling Management Through Sciences and Humanities”, Organized by Alipurduar University, 22nd and 23rd March, 2021. (*Presented a Paper*)
- Annual Convention of Chemists and International Conference on Recent Trends in Chemical Sciences, 21st – 24th December, 2021. (*Participation*)
- SERB Sponsored KARYASHALA, on a Hands-on training Program on Design, synthesis, characterization and understanding of smart functional materials through experimental and computational modelings, by Dept. of Chemistry, University of North Bengal, Darjeeling, (04th July– 11th July, 2022), (*Participation*)
- Science Academies Lecture Workshop on “ New Facets in Chemical Sciences: Challenges and Opportunities” from 22-23rd March 2024 organized by the Department of Chemistry, University of North Bengal, Darjeeling 734013. (*Participation*)